Applied Surface Science 440 (2018) 35–41

Contents lists available at ScienceDirect

Applied Surface Science

journal homepage: www.elsevier.com/locate/apsusc

Full Length Article

Probing interfacial electronic properties of graphene/$CH_3NH_3PbI_3$ heterojunctions: A theoretical study

Jisong Hu [a], Gepeng Ji [a], Xinguo Ma [a,b,*], Hua He [a,b], Chuyun Huang [a,b]

[a] School of Science, Hubei University of Technology, Wuhan 430068, China
[b] Hubei Collaborative Innovation Center for High-efficiency Utilization of Solar Energy, Hubei University of Technology, Wuhan 430068, China

ARTICLE INFO

Article history:
Received 5 September 2017
Revised 6 December 2017
Accepted 29 December 2017
Available online 6 January 2018

Keywords:
Perovskite solar cells
Heterojunction
First-principles
Energy band modulation

ABSTRACT

Interfacial interactions and electronic properties of graphene/$CH_3NH_3PbI_3$ heterojunctions were investigated by first-principles calculations incorporating semiempirical dispersion-correction scheme to describe van der Waals interactions. Two lattice match configurations between graphene and $CH_3NH_3PbI_3$(001) slab were constructed in parallel contact and both of them were verified to form remarkable van der Waals heterojunctions with similar work functions. Our calculated energy band structures show that the Dirac-cone of graphene and the direct band gap of $CH_3NH_3PbI_3$ are still preserved in the heterojunctions, thus graphene can be a promising candidate either as a capping or supporting layer for encapsulating $CH_3NH_3PbI_3$ layer. It is identified that the Schottky barrier of graphene/$CH_3NH_3PbI_3$ heterojunctions can be controlled by the interlayer distance and affected by the stacking pattern of graphene and $CH_3NH_3PbI_3$. The 3D charge density differences present the build-in internal electric field from graphene to $CH_3NH_3PbI_3$ after interface equilibrium and thus, a low *n*-type Schottky barrier is needed for high efficient charge transferring in the interface. The possible mechanism of the band edge modulations in the heterojunctions and corresponding photoinduced charge transfer processes are also described.

1. Introduction

Perovskite solar cells (PSCs), an intriguing class based on dye-sensitized solar cells, have attracted worldwide attention for their impressive power conversion efficiencies and promising potential applications [1,2]. In 2009, first hybrid organic/inorganic halides $CH_3NH_3PbX_3$ (X = Br, I) was introduced as light harvesters in dye-sensitized solar cells with an expected photoconversion efficiency of 3.81% [3]. From then on, a surge of solar cell researches were stimulated for the strong light absorption and high carrier mobility of the perovskite materials [2–5]. In the past few years, the power conversion efficiencies of the PSCs have been improved rapidly by chemical doping or formation of heterojunction composite. For example, Sn doping enhances the light absorption capacity of $CH_3NH_3PbI_3$ ($MAPbI_3$) perovskite materials, so that the short-circuit current density of PSCs increases from 13.3×10^{-3} to 19.1×10^{-3} A/cm^2 [6]. Zhou et al. [7] proposed a $MAPbI_3/TiO_2$ micro heterojunction solar cell with 19.3% photoelectric conversion efficiency. The typical structure of PSCs is a layered structure with TiO_2 layer as electron transport layer as well as $MAPbI_3$ as hole transport layers [7,8]. Nevertheless, the different power conversion efficiency achieved by various synthetic methods implies the complexity and importance of the interface structure in efficient charge separation [9].

Part of π-conjugation delocalized materials are widely applied to investigate electron-transfer processing for their rapid separation of photoinduced carriers, which could be combined with other semiconductors via surface hybridization method to enhance performances, such as graphene, C_{60}, and polyaniline [10–12]. Especially, it is widely regarded that graphene is an electron collector and transporter, which can be used to boost performance of various energy conversion and storage devices [13], or to be a dispersible carrier for catalysts [14]. Zhu et al. [15] reported on the insertion of an ultrathin graphene quantum dots layer between perovskite and TiO_2 to accelerate the electron transfer with 90–106 ps, arguably by optimizing the interfacial morphology. Agresti et al. [16] also performed the addition of graphene and related 2D materials into PSCs, leading to improvements of the power conversion efficiency. Most recently, high performance hybrid photodetector was studied based on graphene and perovskite thin film, which has a responsivity of 180 A W^{-1} [17]. These devices marry graphene's unique properties in terms of high

* Corresponding author at: School of Science, Hubei University of Technology, Wuhan 430068, China.
E-mail address: maxg2013@sohu.com (X. Ma).

https://doi.org/10.1016/j.apsusc.2017.12.260
0169-4332/

carrier mobility with perovskite's optoelectronic properties, i.e., high absorption cross-section and long carrier lifetime [16–19], yielding a large photocurrent and a high quantum efficiency. These researches imply the interfacial interactions are very complicated and the mechanism of interfacial electron transfer process remains unclear, thus it is important to investigate the structural, electronic properties of various graphene-based interfaces in PSCs.

With extensive experimental progress, previous some computational studies have been performed on graphene-based interfaces in PSCs. It is clearly pointed out by Volonakis and Giustino [20], using first-principles calculations, that the introduction of graphene leads to a nanoscale ferroelectric distortion with a permanent polarization of 3 mC/m^2 in graphene/$MAPbI_3$ interfaces, which increases the stability of the $MAPbI_3$ and drives electron extraction from the perovskite and hinders electron–hole recombination. Du et al. [21] confirmed from an ab initio molecular dynamics simulation that the stability of methylammonium lead triiodide in water environment could be maintained via the graphene-coated strategy. It is well known that there are two important aspects to be considered for interface properties of heterojunctions. One is the lattice match between the two components, which is the prerequisite for fabricating heterojunctions; the other is the suitable conduction band (CB) and/or valence band (VB) position, which are considered to be the prime and fundamental requirement for photoinduced charge transfer and separation in the heterojunctions. Thus, comparing with the progress in experimental fabrication of graphene/$MAPbI_3$ heterojunction, its underlying characteristics of the interlayer interaction with different stacking patterns and roles of graphene from a theoretical point of view are not still explained clearly, in particular explicitly considering the correctly van der Waals (vdW) interactions. In this work, to mimic such experimental observations in real time and at the atomistic level, first-principles calculations on the graphene/$MAPbI_3$ heterojunctions with two stacking patterns were employed firstly to explore the basic mechanisms of interface interaction, charge transfer and separation, and band modulation. We finally present a fully coherent picture of the interface properties, which can provide necessary reference for further optimizing performance of heterojunctions. Alkali metal (or transition metal) groups in the graphene/$MAPbI_3$ maybe contribute to a certain extent, although we will not discuss such effects here, and it will be the subject of future work.

2. Calculation methods and models

All calculations were accomplished using the ultrasoft pseudopotentials (USP) with the exchange and correlation in the Perdew-Burke-Ernzerhof (PBE) [22] formalisms of density functional theory (DFT) as implemented in the CASTEP code [23]. In USP calculations, to describe correctly vdW interactions, a hybrid semiempirical solution from Tkatchenko and Scheffler (TS) scheme was given to introduce damped atom pairwise dispersion corrections of the form C_6R^{-6} in the DFT formalism [24]. The dispersion-corrected total energy E_{tot} is represented as

$$E_{total} = E_{KS\text{-}DFT} + E_{vdW} \quad (1)$$

where $E_{KS\text{-}DFT}$ is the conventional Kohn-Sham DFT energy and E_{vdW} is the missing dispersion contribution. The semiempirical approach provides the best compromise between the cost of first-principles evaluation of the dispersion terms and the need to improve nonbonding interactions in the standard DFT description. The valence atomic configurations are $2s^22p^2$ for C, $1s^1$ for H, $2s^22p^3$ for N, $5d^{10}6s^26p^2$ for Pb, $5s^25p^2$ for I, respectively. A cutoff energy of 500 eV and a Monkhorst-Pack grid of $4 \times 8 \times 1$ for Model A and $8 \times 8 \times 1$ for Model B are used, respectively [25]. All results are fully converged with the denser meshes. Geometry optimizations were done with the self-consistent convergence accuracy of 1×10^{-5} eV/atom. The convergence criterion for the maximal force on atoms is 0.05 eV/Å. The maximum displacement is 1×10^{-3} Å, and the stress is less than 0.05 GPa.

The tetragonal $MAPbI_3$ (space group: $I4/mcm$) for room temperature phase is selected, in which each cell contains four repeated $MAPbI_3$ units with a total of 48 atoms. The fixed values $a = b =$ 0.880 nm, $c = 1.269$ nm are taken for the initial lattice constants from the experimental data [26]. Recently, Haruyama et al. [27] confirmed that both terminations can coexist especially, namely, the more probably (110) and (001) surfaces. We identified that the $MAPbI_3$ (001) surface was easier to form than the (110) surface (see Fig. 1S in supporting information (SI)). Here, the $MAPbI_3$(001) surface is only chosen to study their interaction with graphene. The initial CH_3NH_3 configuration is determined by our previous study [28]. Considering the stacking patterns of graphene on the surface of the $MAPbI_3$ with different angles, the most likely two periodic structures of graphene, namely, graphene I (quadrangle ABCD) and graphene II (quadrangle DEFG) are selected to match the lattice constants of the $MAPbI_3$(001) surface. Compared with graphene I, the angle of the stacking structure of graphene II has the deflection of 16.1 degrees, as shown in Fig. 1a. For Model A, a 1×2 supercell surface of $MAPbI_3$(001) surface is constructed as the substrate to match graphene I sheet, as shown in Fig. 1b. For Model B, the 1×1 surface of $MAPbI_3$(001) is chose to match graphene II sheet, as shown in Fig. 1c. A vacuum layer of 15 Å is used to isolate the slab as the boundary condition, which according to other previous work, is good enough to make interactions between neighbouring slabs negligible.

3. Results and discussion

It is well known that the interlayer interaction will affect directly the interface structure stability of the fabricated heterojunctions. To investigate the thermodynamic stability of the graphene/$MAPbI_3$ heterojunctions, the interface cohesive energy was taken as follow

$$E_{coh} = [E(\text{hetero}) - E(\text{graphene}) - E(MAPbI_3(001))]/A \quad (2)$$

where E(hetero), E(graphene) and $E(MAPbI_3(001))$ represent the total energies of the relaxed graphene/$MAPbI_3$(001) heterojunction,

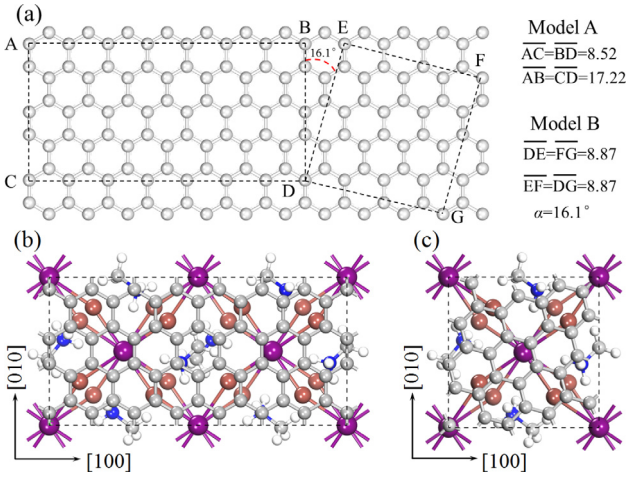

Fig. 1. Two stacking patterns of the graphene/$MAPbI_3$(001) heterojunctions. (a) The geometric relation between graphene I and graphene II. Top view of stacking pattern of (b) Model A and (c) Model B. Purple, orange, gray, blue, and white balls represent Pb, I, C, N and H atoms, respectively. (For interpretation of the references to colour in this figure legend, the reader is referred to the web version of this article.)